International Journal of Mass Spectrometry 430 (2018) 87–97

Contents lists available at ScienceDirect

International Journal of Mass Spectrometry

journal homepage: www.elsevier.com/locate/ijms

PTR-ToF-MS product ion distributions and humidity-dependence of biogenic volatile organic compounds

Eetu Kari[a,*], Pasi Miettinen[a], Pasi Yli-Pirilä[b], Annele Virtanen[a], Celia L. Faiola[a,c]

[a] Department of Applied Physics, University of Eastern Finland, P.O. Box 1626, 70211 Kuopio, Finland
[b] Department of Environmental and Biological Sciences, University of Eastern Finland, P.O. Box 1627, 70211 Kuopio, Finland
[c] Department of Ecology and Evolutionary Biology, University of California Irvine, Irvine, CA 92967-2525, USA

ARTICLE INFO

Article history:
Received 12 December 2017
Received in revised form 28 March 2018
Accepted 2 May 2018
Available online 4 May 2018

Keywords:
PTR-ToF-MS
Product ion distribution
Monoterpene
Sesquiterpene
Humidity-dependence
BVOC

ABSTRACT

Quantitative proton-transfer-reaction mass spectrometer (PTR-MS) measurements of ambient volatile organic compounds (VOCs) require proper calibration procedures. In particular, compound product ion distribution and humidity-dependent responses must be characterized. In this study, we generated twelve gas-phase terpenoid standards using a dynamic dilution system to calibrate the PTR-MS with time-of-flight mass spectrometer (PTR-ToF-MS): six monoterpenes, two monoterpene derivatives, and four sesquiterpenes. The humidity-dependent response was characterized for three terpenoid compounds to compare different molecular structures: α-pinene, δ-limonene, and longifolene. We provide the first comprehensive summary of PTR-ToF-MS product ion distributions for twelve common biogenic volatile organic compounds using two different reduced electric field (E/N) values, 80 Td and 130 Td. Results demonstrated that neglecting to correct for individual product ion distributions of different terpenoid isomers can result in an error of up to 26% for reported mixing ratios. δ-Limonene and longifolene exhibited a small humidity-dependent response in the PTR-ToF-MS, but this did not contribute significantly to the overall measurement error. These results will improve quantification of commonly-measured biogenic volatile organic compound emissions and chemistry in the atmosphere.

© 2018 The Authors. Published by Elsevier B.V. This is an open access article under the CC BY license (http://creativecommons.org/licenses/by/4.0/).

1. Introduction

Proton-transfer-reaction mass spectrometers (PTR-MSs) are commonly used for real-time monitoring of volatile organic compounds (VOCs) in air, including highly reactive monoterpenes ($C_{10}H_{16}$) and sesquiterpenes ($C_{15}H_{24}$) emitted from forests [1–7]. One of the advantages of the PTR-MS is the ability to detect many trace VOCs with high sensitivity and low limit of detection. Despite the soft ionization technique used in the PTR-MS, many of the VOCs, including monoterpenes and sesquiterpenes, fragment substantially due to energetic collisions in the drift tube [8–11]. The product ion distributions resulting from fragmentation are dependent on the reduced electric field (E/N) in the drift tube and the compound molecular structure. Several different isomers of mono- and sesquiterpenes having different molecular structures are continuously emitted by forests. This presents an analytical problem because the isomers cannot be distinguished with the PTR-MS, and the different isomers can fragment into several masses based on their physico-chemical properties and molecular structure. To accurately measure ambient mixing ratios of a mixture of mono- and sesquiterpenes, the PTR-MS must be calibrated against the same terpenoid compounds that are measured from the ambient air. Quite frequently, PTR-MS instruments are calibrated with only one monoterpene, especially when a calibration gas is used for calibration purposes [4–7,12]. This is because many mono- and sesquiterpenes are not readily available in standard gas cylinders and/or the cost is prohibitively expensive. However, limited molecular representation could introduce quantification errors when the ambient terpene profile consists of different isomers from those in the calibration gas. In this paper, we present a comprehensive summary of product ion distributions for twelve terpenoid compounds: six monoterpenes, two structural derivatives of monoterpenes (*p*-cymene and 1,8-cineole), and four sesquiterpenes. Gas-phase standards of each compound were generated using a dynamic dilution system [13]. The product ion distributions were measured for each compound at two E/N settings: 80 Td and 130 Td (Td = Townsend, 1 Td = 10^{-17} V cm^2). To our knowledge, this is the first detailed report of the product ion distributions for several terpenoid biogenic VOCs (BVOCs) in the PTR-MS with a time-of-flight mass spectrometer (PTR-ToF-MS). Product ion distributions

* Corresponding author at: Department of Applied Physics, University of Eastern Finland, P.O. Box 1627, 70211 Kuopio, Finland.
E-mail addresses: eetu.kari@uef.fi (E. Kari), pasi.miettinen@uef.fi (P. Miettinen), pasi.yli-pirila@uef.fi (P. Yli-Pirilä), annele.virtanen@uef.fi (A. Virtanen), cfaiola@uci.edu (C.L. Faiola).

https://doi.org/10.1016/j.ijms.2018.05.003
1387-3806/© 2018 The Authors. Published by Elsevier B.V. This is an open access article under the CC BY license (http://creativecommons.org/licenses/by/4.0/).

were reported previously using the PTR-MS with a quadrupole mass spectrometer (PTR-Q-MS) for monoterpenes by Tani et al. and for sesquiterpenes by Kim et al. and Demarcke et al. [8–10]. However, ion transmission is different through time-of-flight and quadrupole mass spectrometers, and the duty cycle of the PTR-ToF-MS enhances the detection of heavier ions at the cost of lighter ions [14]. These differences suggest that product ion distributions would also differ between PTR-ToF-MS and PTR-Q-MS instruments. Hence, the product ion distributions reported here fill a critical gap for many PTR-ToF-MS users who measure BVOC emissions and chemistry. In addition to product ion distribution considerations, some mono- and sesquiterpenes exhibit a humidity-dependent response in the PTR-MS depending on their structure [8,10,15]. In this study, we explored the humidity-dependent response of the PTR-ToF-MS for three compounds with different structures: α-pinene, δ-limonene, and longifolene. These three compounds were selected because they were the focus of earlier investigations using the PTR-Q-MS [8,10,15], and therefore, provided a comparison of humidity-dependent responses between the two analytical systems.

Ionization of the sample in a PTR-MS occurs through proton-transfer reactions with H_3O^+ ions. Proton-transfer reactions produce RH^+ ions, and the concentration of the analyte, R, can be calculated using Eq. (1) [16].

$$\left[RH^+\right] \approx [H_3O^+]_0 \cdot k \cdot [R] \cdot \Delta t \quad (1)$$

where $[H_3O^+]_0$ is the concentration of reagent ions introduced from the ion source, k is the rate constant for the proton-transfer reaction, [R] is the concentration of trace gas R, and Δt is the reaction time of the ions. This approximation is justified if H_3O^+ ions are excessively present in the drift tube, which is the case with the PTR-MS [16].

Using Eq. (1) to quantify VOCs without further corrections can lead to several quantification errors. For example, one source of error originates from using a standard value of $2{\cdot}10^{-9}$ cm^3 s^{-1} for the rate constant, k, because even the use of an experimentally determined value for k may result in an error margin of 50% for the rate constant [1]. Such a high error margin is due to elevated effective temperature conditions in the drift tube. Other potential sources of error in Eq. (1) include the uncertainty in the transit time of ions through the drift tube and variation in ion transmissions as a function of m/z. This variation must be determined before every measurement campaign, which is typically done using a gas cylinder containing several compounds with varying masses that do not fragment inside the PTR-MS, for example different aromatic compounds. In addition, Keck et al. have shown that H_3O^+ ions and protonated VOCs lack equal mobility, contrary to one of the assumptions used to derive Eq. (1), which can lead to errors greater than 20% [17]. In addition to quantitative errors associated with Eq. (1), PTR-MS response to different VOCs depends on the efficiency of the instrument to collect and detect the analyte, and on the extent to which the reactions between H_3O^+ ions and VOCs are taking place in the drift tube [18]. Moreover, if the VOC has only slightly higher proton affinity (PA) than water, reverse proton-transfer reactions can occur. This is the case for example with formaldehyde [19]. Consequently, the response of the PTR-MS to these compounds is significantly lower compared to other VOCs that have clearly higher PAs than water. These sources of error highlight the importance of careful PTR-MS calibration.

Different approaches exist for PTR-MS calibration to account for the sources of error described above. One of the most commonly used calibration methods is using a multi-component standard gas cylinder that is dynamically diluted with clean air [4–7,12]. Other methods include diffusion systems [8] and permeation tubes [11,20–23]. Diffusion systems operate by continuously diffusing the vapor of a standard compound into an air stream. Usually, a small amount of the standard is placed in a vial and the vial's cap is pierced with a small tube through which the diffusion takes place. Once the diffusion rate of the standard is known it can be diluted with another air stream to the desired mixing ratio for calibration purposes. The use of permeation tubes requires knowledge about the permeation rate of the standard through a porous permeation tube at temperature controlled conditions. The permeation rate of a standard can be calculated by weighing the permeation tube periodically. Once a constant permeation rate is achieved the desired mixing ratios can be prepared by diluting the standard permeating through the tube. Additionally, Ionicon Analytik, the manufacturer of many PTR-MS instruments used by several research groups, sells a liquid calibration unit (LCU) that nebulizes aqueous standards to evaporate them into a stable gas stream. This system was designed specifically for PTR-MS calibration purposes [24].

All the calibration methods described above have their strengths, but they also have weaknesses that limit their utility. Some of these methods require the preparation of pure standards prior to calibration (LCU) [24], some methods are time-consuming (preparation of permeation tubes) [11,25,26], and others are expensive (permeation tubes, gas cylinders) [25,27]. Moreover, the lifetimes of the gases in cylinders are limited. Hence, VOCs may start to degrade in cylinder so they cannot be used anymore for calibration purposes, and the purchase of a new cylinder is necessary [27,28]. In addition, one significant disadvantage with gas cylinders used for PTR-MS calibration is that one cylinder can contain only one isomeric compound like monoterpenes, due to the limitation of the PTR-MS to distinguish isomeric compounds. Therefore, the calibration of the PTR-MS against many different VOC isomers requires the purchase of more than one gas cylinder, raising costs.

Due to the main disadvantages (cost, time, standard preparation) of existing PTR-MS calibration systems, we used a dynamic dilution system—a cost-effective and simple option to calibrate the PTR-MS, and to determine product ion distributions for the studied terpenoid compounds. The basic idea behind the dynamic dilution system is presented in Faiola et al. and described again here [13]. The pure liquid standard is infused continuously into a heated air stream with a precisely known infusion rate using a syringe pump. The standard evaporates quickly as it is introduced to the heated air stream to produce stable, reproducible, and quantitative gas-phase VOC standards. We generated gas-phase standards for twelve different terpenoid compounds with the dynamic dilution system to quantify product ion distributions for two different reduced electric field (E/N) settings. To our knowledge, this is the first publication of PTR-ToF-MS product ion distributions for these important terpenoid BVOCs. Furthermore, a sub-set of the standards was used to investigate humidity-dependent responses of the PTR-ToF-MS for three terpenoid compounds to compare humidity-dependence between the PTR-ToF-MS and the PTR-Q-MS. These results provide useful information to PTR-ToF-MS users that will improve analytical quantification of BVOC measurements.

2. Experimental

2.1. Dynamic dilution system

VOC standards were generated by diluting pure liquid standards with the purified air flow that was introduced into the system via a mass flow controller (MFC, Aalborg, model GFC17). By changing the infusion rate of the liquid standard, we were able to generate VOC mixing ratios from 5 ppb to 200 ppb—the range that was desired for this study.

The system was modified from the dynamic dilution system constructed by Faiola et al. by adding the humidification option [13]. As

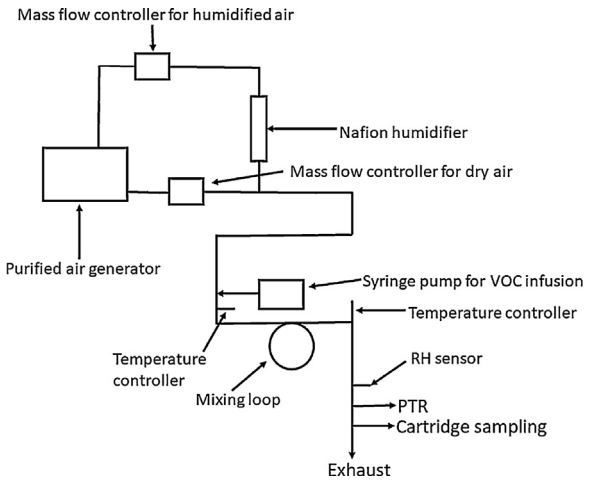

Fig. 1. The schematic of the dynamic dilution system.

previously described by Faiola et al. the system consisted of heated air flow, the VOC injection system, and a mixing loop to homogeneously mix the standard with the dilution gas (Fig. 1) [13]. In addition to that, as Fig. 1 shows we added to the system an option to humidify the dilution air that enabled calibrations under a range of humidity conditions.

The dynamic dilution system was made of stainless steel tubing (o.d.=6 mm) surrounded by heat tape and insulation to ensure approximately equal temperature throughout the system. The system was constructed of stainless steel compression fittings with stainless steel ferrules (Swagelok, Inc.). The compounds were introduced to the system with a microliter syringe (Hamilton, model CTC 5 μl, and ILS 1 μl SYR T were used in this study) inserted through a septum on a tee fitting. The infusion rate of the standard was controlled by a syringe pump (Chemyx Inc., model Nexus 3000) with highly accurate low flow rates on the order of nL h^{-1}. The mixing ratios of the compounds were calculated by Eq. (2).

$$Mixing\ ratio\,[\mathrm{ppb}] = \frac{infusion\ rate \cdot \rho \cdot 10^9}{M \cdot molar\ flow} \quad (2)$$

where ρ and M were the density and molecular weight of the liquid standard, respectively.

The system was kept at a constant temperature that was chosen based on the vapor pressure of the standard compound. To maintain the desired temperature of the system, the air flow was heated by heat tape (Oy Meyer vastus Ab, Finland), and the temperature was controlled with PID temperature controllers (Oy Meyer vastus Ab, Finland). The choice of temperature was critical because the liquid standard would evaporate too quickly in the syringe needle (if temperature was too high) resulting in highly variable output mixing ratio, or liquid droplets would be introduced to the system (if temperature was too low) generating unpredictable bursts of increased mixing ratios. The temperature setting for the monoterpenes, *p*-cymene and 1,8-cineole was 45 °C and for sesquiterpenes was 60 °C.

The humidity of the air flow was adjusted with a Model PD-200T-12MSS (Perma Pure, LLC, USA) humidifier. The dry and humid air were mixed upstream of VOC infusion. Relative humidity (RH) of the dilution air was measured with a humidity probe (Vaisala HMP 110 0-100% RH) that was attached to a Swagelok tee upstream of the inlet line of the PTR-ToF-MS (Fig. 1).

2.2. PTR-ToF-MS and compounds for calibration

A detailed description of the PTR-MS has been given in several publications [1,16,29]. Consequently, only key details are described in this paper. The PTR-ToF-MS consists of four main parts: 1) a hollow cathode discharge ion source, where H_3O^+ ions are generated from water vapor; 2) a drift tube reaction chamber, where the VOCs from the sample air are introduced and ionized by proton-transfer reactions with H_3O^+ ions; 3) a transfer lens system, which guides the newly-formed ions into the mass spectrometer; and 4) a reflectron time-of-flight mass spectrometer, where the ionized compounds are separated with high mass resolution based on their mass-to-charge ratios. The ions are detected by a multi-channel plate detector.

Many of the trace VOCs in the atmosphere can be detected with the PTR-MS because they possess PAs higher than that of water. In this case the proton-transfer reactions proceed at the collision rate of about 1–4·10^{-9} cm^3 $molecule^{-1}$ s^{-1} [30]. After proton-transfer reactions occur, the ions are transported over the length of the drift tube by the electric field. The high electric field reduces clustering of the reagent and product ions with water because the average kinetic energy of the ions is increased. In addition to the applied electric field, E, the density of gas in the drift tube, N, also affects the energy brought to the de-clustering collisions [3]. The ratio of E/N is called the reduced electric field. While the reduced electric field minimizes clustering, it promotes fragmentation. Higher E/N values lead to a higher number of energetic collisions inside the drift tube that increases the degree of VOC fragmentation.

The compounds used in this study for the PTR-ToF-MS (PTR-TOF 8000, Ionicon Analytik, Austria) calibration are shown in Fig. 2; for this study we chose six monoterpenes, two monoterpene derivatives, and four sesquiterpenes. The PTR-ToF-MS sampled the VOCs with a known mixing ratio from the outlet of the dynamic dilution system, through 60 °C heated PEEK (I.D. 1 mm) tubing. The instrument was operated in the following conditions: drift tube pressure and temperature were set to 2.30 mbar and 60 °C, respectively. The instrument was operated with two E/N values; the drift tube voltage was changed between 350 V and 600 V in order to reach E/N values of 80 Td and 130 Td in the drift tube. The signals were corrected for instrumental transmission coefficients by using a standard gas cylinder (BOC, UK) containing 8 different aromatic VOCs that had nominal masses ranging from 78 amu (benzene) to 181 amu (trichlorobenzene). The data were analyzed by PTR-MS Viewer version 3.2 (Ionicon Analytik, Austria).

3. Results and discussion

3.1. Dynamic dilution system characterization

The dynamic dilution system was characterized to ensure it was working properly before using it for PTR-MS calibrations. First, we confirmed that the system was producing gas-phase standards with theoretical mixing ratios based on Eq. (2) by validating it against a well-established off-line GC–MS analytical technique. During α-pinene and *p*-cymene standard generation, we collected duplicate adsorbent cartridge samples (Tenax TA/Carbograph 5TD, MARKES international, United Kingdom) for 5 calibration points (10, 20, 50, 100, 200 ppb) and compared theoretical to observed mixing ratios. Cartridge samples were analyzed off-line using a thermal desorption-gas chromatography-mass spectrometer (TD-GC–MS, TD: Perkin Elmer, ATD 400, USA, GC–MS: Hewlett Packard, GC 6890, MSD 5973, USA). For GC we used HP-5MS UI column the length of 60 m (d = 0.250 mm, film thickness = 0.25 μm, Agilent Technologies, USA). Fig. 3 shows the comparison of theoretical to observed mixing ratios in a scatter plot. The slopes of the linear fits in Fig. 3 demonstrate that the observed mixing ratios were in good agreement with the theoretical values. More specifically, the errors of individual datapoints varied between 0.2% and 5.2%: for α-pinene the errors were −0.5% (10 ppb), 4.0% (50 ppb), 1.5% (100 ppb), 2.3% (150 ppb),

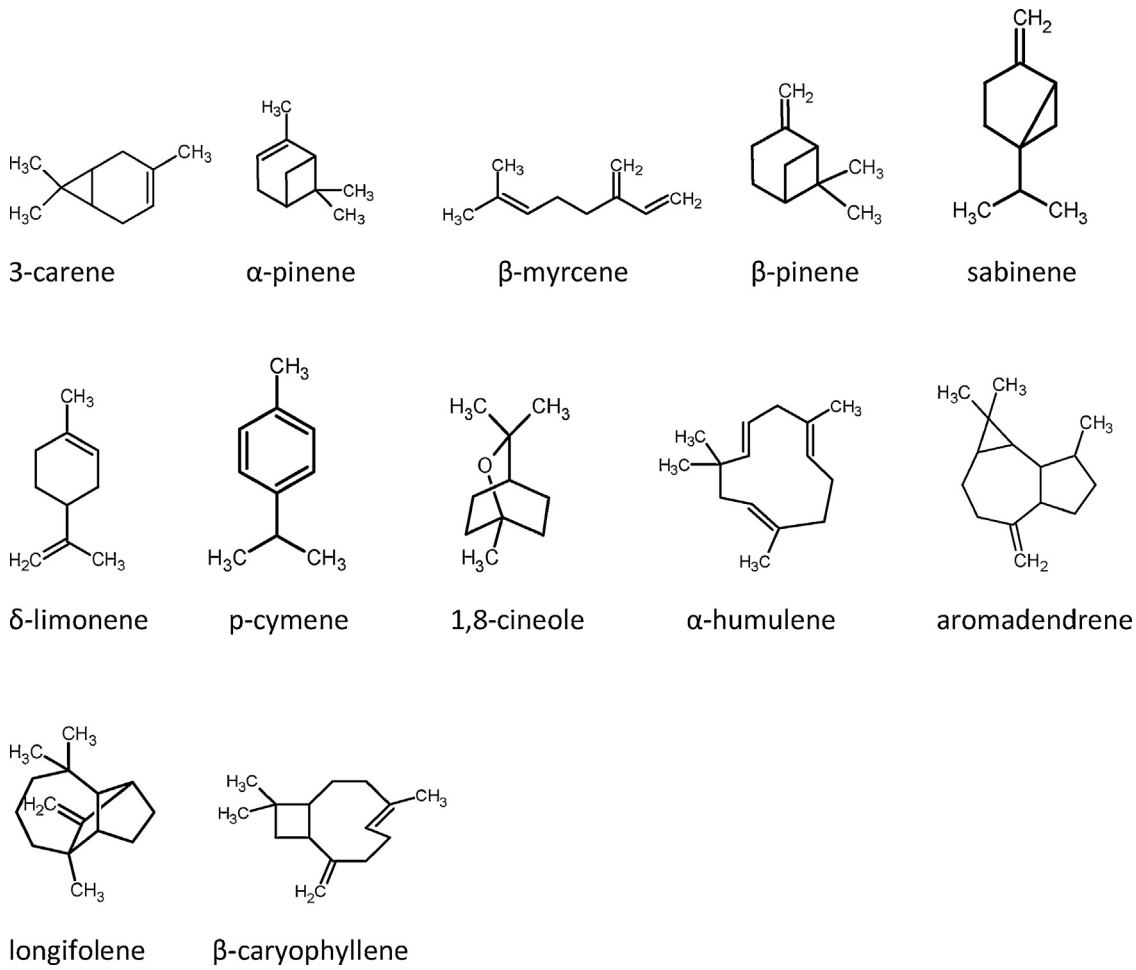

Fig. 2. Molecular structures of terpenoid compounds studied in this work.

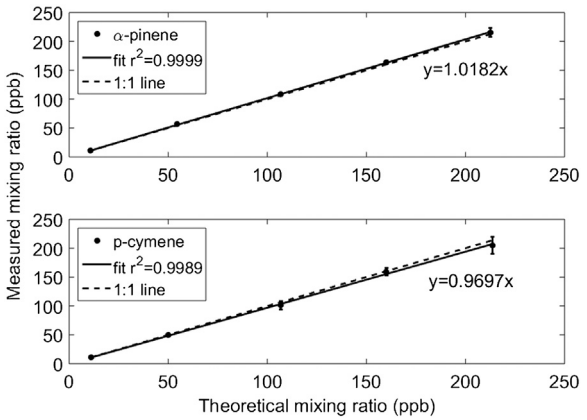

Fig. 3. Dynamic dilution system generated mixing ratios as a function of theoretical mixing ratios for α-pinene (upper panel) and *p*-cymene (lower panel). System generated mixing ratios were collected to cartridges and analyzed by TD-GC–MS. Black solid lines (fit) shows linear regression fits, and slope shows how well measured and theoretical mixing ratios were agreeing with each other.

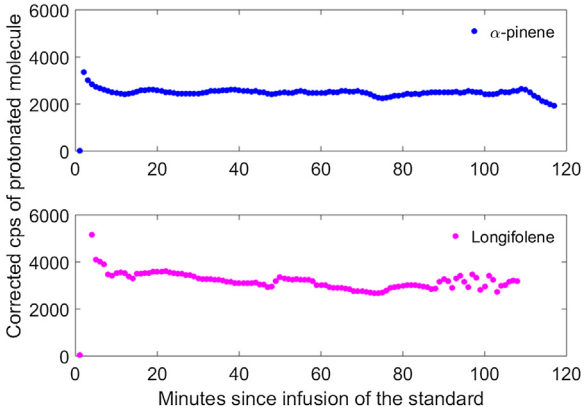

Fig. 4. The equilibration period and stability of the protonated molecule of α-pinene (*m*/*z* 137.13) and longifolene (*m*/*z* 205.20) standards generated by the dynamic dilution system. The data is averaged to one minute.

and 1.5% (200 ppb), and for *p*-cymene the errors were −2.5% (10 ppb), −0.2% (50 ppb), −5.2% (100 ppb), −0.6% (150 ppb), and −4.0% (200 ppb). Negative error indicates that the theoretical mixing ratio was higher than the observed one. The differences between theoretical and observed mixing ratios could be attributed to errors in the accuracies of the syringe pump and mass flow controller, and to a lesser degree in the cartridge sampling, and TD-GC–MS analysis.

The second characterization step was to verify the stability of the signal because the gas-phase standard mixing ratios needed to be stable for enough time to ensure an accurate and reliable calibration of the PTR-MS. We tested stability of the system with α-pinene and longifolene standards by monitoring the variation in signal after the system reached equilibrium. Fig. 4 shows that equilibrium was reached in 15 min for α-pinene, and in 30 min for longifolene, due to the lower vapor pressure of the latter. After reaching equilibrium, the PTR-MS signal of the protonated molecule, in units of corrected

counts per second (cps), stayed constant for approximately 65 min at 50 ppb of α-pinene and 40 min at 35 ppb of longifolene (Fig. 4). The stability of the signal was tested with Mann-Whitney *U* test. PTR-MS signal was corrected for the instrument's transmission, and the saturated primary ion ($H_3{}^{16}O^+$) cps values were calculated using the primary ion isotope ($H_3{}^{18}O^+$) multiplied by a factor of 500, which was determined from the isotope ratio. Relative standard deviations of corrected cps values were 3.1% for α-pinene and 5.5% for longifolene.

Additional evidence that the dynamic dilution system was working well for PTR-MS calibration is provided in Fig. 5, which presents the calibration curves for all studied compounds. Fig. 5 shows that all calibration curves have coefficient of determination (r^2) close to 1, indicating the quantitative dynamic range of the dynamic dilution system. Furthermore, the small errors bars (1 standard deviation) of the corrected cps values demonstrate the stability of the mixing ratios generated by the dynamic dilution system.

3.2. Calibration of PTR-ToF-MS

The PTR-ToF-MS was calibrated for six monoterpenes, two structural derivatives of monoterpenes, and four sesquiterpenes (see Fig. 2). The calibration curves of the protonated molecules are presented in Fig. 5. Fig. 5 shows that most of the calibration curves of monoterpenes and monoterpene derivatives (left panel of Fig. 5) have similar slopes ranging from 65.1 ± 0.7 corrected cps/ppbv for α-pinene to 77.3 ± 0.7 corrected cps/ppbv for 1,8-cineole (the slopes of the calibration curves are reported with 95% confidence intervals). However, *p*-cymene and limonene have clearly smaller slopes (29.6 ± 0.5 corrected cps/ppbv and 29.6 ± 1.8 corrected cps/ppbv, respectively) than other monoterpenes, which means that these two compounds undergo more fragmentation inside the drift tube of PTR-MS at 130 Td (more details in Sect. 3.3 about fragmentations). For sesquiterpenes (right panel of Fig. 5) the slopes were more variable between isomers, ranging from 37.8 ± 3.1 corrected cps/ppbv for *trans*-caryophyllene up to 88.8 ± 14.5 corrected cps/ppbv for longifolene. This variability is due to more substantial differences in fragmentation between the different sesquiterpenes. This result highlights the importance of conducting calibrations using the same compounds as those included in the analyte mixture because the degree of fragmentation of the protonated molecule is different for each compound (more details in Sect 3.5 about the importance of doing calibrations with the proper compounds). Hence, to correct the mixing ratios measured by the PTR-MS reliably, the calibration factors must be determined separately for each compound studied.

3.3. Product ion distributions of monoterpenes and sesquiterpenes

The reduced electric field applied to transfer ions through the drift tube causes fragmentation of the protonated molecules. The degree of fragmentation depends on the value of E/N; the greater E/N, the greater fragmentation because of the increased number of energetic collisions taking place inside the drift tube. Fragmentation patterns create unique product ion distributions, which have been reported in the PTR-Q-MS for several monoterpenes and sesquiterpenes [8–10]. However, transmission coefficients, and thus product ion distributions, of the PTR-MS depend on the type of mass spectrometer used, so updated information is required for PTR-ToF-MS users. Transmission coefficients of the ions of different masses depend on the transmission efficiency of the instrument for these ions. Transmission efficiency refers to the fraction of ions that reach the detector and is dependent on the ion mass. This ion loss is caused by unstable ion trajectories, collisions of ions with the solid parts of grid electrodes, imperfect performance of ion lenses, and the scattering of ions by residual background gas molecules [3]. Additionally, the mass analyzer used inside the mass spectrometer affects the shape of the transmission curve (transmission efficiency of ions with different masses) determining which ions are transported to the detector with the highest abundance [31].

Table 1 shows the product ion distributions of twelve different terpenoid compounds for two reduced electric field settings calculated for corrected cps values (left side of Table 1) and for uncorrected cps values (right side of Table 1). The fragment abundance was calculated from total corrected cps and total uncorrected cps values. The contribution from the ions in Table 1 includes the sum of its corresponding isotopes. Table 1 only includes the product ions for each compound with corrected cps values of the non-isotopic ion covered more than 1% from the total corrected cps values produced by the VOC. The exception was 1,8-cineole, whose protonated molecule ($C_{10}H_{19}O^+$, *m/z* 155) abundance is reported even though it comprised less than 1% of the total corrected cps signal at 130 Td. This exception was made to illustrate that the protonated molecule of 1,8-cineole was present, and it did not fragment completely even in a high energy electric field. The product ions were identified and separated from possible impurities using the following approach. First, if the ion followed the temporal concentration profile of the protonated molecule during the whole calibration run including the stabilization period it was identified as a possible product ion of the compound. Second, when the assumed product ion contributed with the same abundance to total cps for each concentration during the whole calibration run it was verified to be the product ion of the compound. With this approach we were able to identify all impurities in the standard, except the isomers of the standard. However, to exclude the possibility that different isomers of the standards would have significantly interfered the determination of the product ion distributions and calibrations, we used very pure standards (≥95%, see Table 1) in this study. Only exception was β-myrcene standard that had a purity of ≥90%. To confirm that impurities did not interfere β-myrcene calibration, we conducted GC–MS analysis for β-myrcene standard to verify that impurities including other monoterpene isomers did not significantly interfere the calibration of β-myrcene. GC–MS analysis showed that β-myrcene covered 93% from all compounds present in the standard. The impurities in the β-myrcene standard were mainly other monoterpenes. Hence, we were able to conclude that other monoterpene isomers in β-myrcene standard did not interfere significantly the calibration of β-myrcene in this study. In addition to GC–MS analysis of β-myrcene, we conducted GC–MS analysis for α-pinene, and *p*-cymene when we characterized the dynamic dilution system (see Sect. 3.1). GC–MS analysis showed that the standards of α-pinene and *p*-cymene contained both less than 1% impurities that were originated from other monoterpenes. Therefore, we can be confident that impurities including mono- or sesquiterpene isomers of other standards did not significantly interfere the calibrations, due to high purity of the standards used in this study.

Table 1 shows that the abundance of protonated molecule increases with decreasing E/N value. This is because a smaller number of energetic collisions occur inside the drift tube with lower E/N value. Table 1 also demonstrates that the molecular structure of the monoterpene determines how much fragmentation takes place inside the drift tube. For example, bicyclic monoterpenes (α-pinene, β-pinene, 3-carene, sabinene, 1,8-cineole) produced mainly one product ion ($C_6H_9^+$, *m/z* 81.07) in addition to protonated molecule ($C_{10}H_{17}^+$, *m/z* 137.13). These two ions covered more than 90% of the total corrected ion counts at both E/N values (Table 1). Like the bicyclic monoterpenes, the most abundant product ion from mono- and acyclic monoterpenes (δ-limonene, β-myrcene) was $C_6H_9^+$ (*m/z* 81.07). In contrast to bicyclic monoterpenes, mono-

Table 1
Manufacturers of studied monoterpenes, monoterpene derivatives, and sesquiterpenes, and their product ion distributions determined for corrected cps and cps values. The contribution from the ions includes the sum of its ^{12}C and ^{13}C isotopes.

Compound (Manufacturer, purity)	Product ions, *m/z*	E/N dependency (corrected cps)		E/N dependency (cps)	
		Abundance (%) at 130 Td	Abundance (%) at 80 Td	Abundance (%) at 130 Td	Abundance (%) at 80 Td
3-carene (Sigma-Aldrich, ≥95%)	67.06 ($C_5H_7^+$)	1.0	–	0.8	–
	81.07 ($C_6H_9^+$)	39.5	23.0	34.6	19.2
	93.07 ($C_7H_9^+$)	5.0	2.6	4.5	2.2
	95.09 ($C_7H_{11}^+$)	2.1	–	1.9	–
	137.13 ($C_{10}H_{17}^+$)	50.9	72.2	56.4	76.1
	151.11 ($C_{10}H_{15}O^+$)	1.5	2.2	1.8	2.5
α-pinene (Sigma-Aldrich, ≥99%)	81.07 ($C_6H_9^+$)	47.7	34.7	42.2	29.6
	93.07 ($C_7H_9^+$)	2.1	1.7	1.9	1.5
	95.09 ($C_7H_{11}^+$)	1.9	–	1.8	–
	137.13 ($C_{10}H_{17}^+$)	48.3	63.6	54.1	68.9
β-myrcene (Sigma-Aldrich, ≥90%)	41.04 ($C_3H_5^+$)	1.3	–	0.8	–
	67.06 ($C_5H_7^+$)	1.4	1.0	1.2	0.8
	69.07 ($C_5H_9^+$)	4.7	3.8	4.0	3.1
	81.07 ($C_6H_9^+$)	32.7	29.0	29.2	25.2
	93.07 ($C_7H_9^+$)	1.9	1.5	1.7	1.4
	95.09 ($C_7H_{11}^+$)	10.9	6.8	10.0	6.1
	137.13 ($C_{10}H_{17}^+$)	47.1	57.9	53.1	63.4
β-pinene (Sigma-Aldrich, ≥99%)	81.07 ($C_6H_9^+$)	48.8	36.5	43.3	31.4
	93.07 ($C_7H_9^+$)	2.1	1.5	1.9	1.3
	95.09 ($C_7H_{11}^+$)	2.4	1.1	2.3	1.0
	137.13 ($C_{10}H_{17}^+$)	46.7	60.9	52.5	66.3
δ-limonene (Sigma-Aldrich, ≥97%)	67.06 ($C_5H_7^+$)	1.0	–	0.9	–
	81.07 ($C_6H_9^+$)	41.0	20.3	36.2	16.8
	93.07 ($C_7H_9^+$)	4.0	2.4	3.7	2.1
	95.09 ($C_7H_{11}^+$)	6.6	3.1	6.0	2.6
	107.09 ($C_8H_{11}^+$)	3.4	2.0	3.4	1.9
	137.13 ($C_{10}H_{17}^+$)	30.9	54.8	34.6	57.3
	151.11 ($C_{10}H_{15}O^+$)	7.2	9.4	8.3	10.4
	153.13 ($C_{10}H_{17}O^+$)	5.9	8.0	6.9	8.9
sabinene (Chemos GmbH, ≥99%)	81.07 ($C_6H_9^+$)	40.8	29.0	35.7	24.5
	93.07 ($C_7H_9^+$)	2.6	1.6	2.3	1.4
	95.09 ($C_7H_{11}^+$)	3.5	1.6	3.1	1.4
	137.13 ($C_{10}H_{17}^+$)	51.6	65.8	57.1	70.4
	151.11 ($C_{10}H_{15}O^+$)	1.5	2.0	1.8	2.3
p-cymene (Fluka, ≥95%)	41.04 ($C_3H_5^+$)	1.6	–	1.0	–
	91.06 ($C_7H_7^+$)	1.8	–	1.7	–
	93.07 ($C_7H_9^+$)	75.5	4.4	72.6	3.6
	119.09 ($C_9H_{11}^+$)	2.2	1.5	2.4	1.5
	135.12 ($C_{10}H_{15}^+$)	18.9	94.1	22.3	94.9
1,8-cineole (eucalyptol) (Fluka, ≥99%)	81.07 ($C_6H_9^+$)	44.4	6.3	38.8	5.0
	95.09 ($C_7H_{11}^+$)	1.5	–	1.3	–
	137.13 ($C_{10}H_{17}^+$)	53.6	84.1	59.3	84.6
	155.14 ($C_{10}H_{19}O^+$)	0.5	9.6	0.6	10.4
α-humulene (Sigma-Aldrich, ≥96%)	41.04 ($C_3H_5^+$)	1.2	1.9	0.6	0.9
	69.07 ($C_5H_9^+$)	3.3	2.3	2.3	1.6
	81.07 ($C_6H_9^+$)	5.5	3.3	4.1	2.4
	95.09 ($C_7H_{11}^+$)	9.9	8.3	7.7	6.2
	109.10 ($C_8H_{13}^+$)	8.2	6.6	7.0	5.5
	121.10 ($C_9H_{13}^+$)	2.1	1.5	1.9	1.3
	123.12 ($C_9H_{15}^+$)	7.7	6.2	7.0	5.5
	135.12 ($C_{10}H_{15}^+$)	4.7	3.9	4.4	3.5
	137.13 ($C_{10}H_{17}^+$)	3.3	3.0	3.2	2.7
	149.13 ($C_{11}H_{17}^+$)	9.0	7.1	8.8	6.8
	205.20 ($C_{15}H_{25}^+$)	43.6	53.8	51.2	61.2
	221.19 ($C_{15}H_{25}O^+$)	1.5	2.1	1.8	2.4
aromadendrene (Sigma-Aldrich, ≥97%)	81.07 ($C_6H_9^+$)	2.5	1.3	1.7	0.9
	95.09 ($C_7H_{11}^+$)	5.0	2.4	3.6	1.7
	109.10 ($C_8H_{13}^+$)	5.0	2.9	4.0	2.2
	121.10 ($C_9H_{13}^+$)	1.1	–	1.0	–
	123.12 ($C_9H_{15}^+$)	3.0	1.5	2.5	1.3
	135.12 ($C_{10}H_{15}^+$)	3.7	2.2	3.2	1.9
	149.13 ($C_{11}H_{17}^+$)	12.9	6.5	11.7	5.6
	205.20 ($C_{15}H_{25}^+$)	66.8	82.1	72.3	85.3
	221.19 ($C_{15}H_{25}O^+$)	–	1.1	–	1.1
longifolene (Fluka, >99%)	81.07 ($C_6H_9^+$)	1.9	1.0	1.2	0.7
	95.09 ($C_7H_{11}^+$)	6.8	4.0	4.5	2.7
	109.10 ($C_8H_{13}^+$)	6.8	3.9	5.0	2.9
	123.12 ($C_9H_{15}^+$)	2.6	1.0	2.1	0.8
	135.12 ($C_{10}H_{15}^+$)	2.4	1.3	2.1	1.1
	149.13 ($C_{11}H_{17}^+$)	8.9	3.8	8.4	3.4
	205.20 ($C_{15}H_{25}^+$)	70.6	85.0	76.7	88.4

Table 1 (*Continued*)

Compound (Manufacturer, purity)	Product ions, *m/z*	E/N dependency (corrected cps)		E/N dependency (cps)	
		Abundance (%) at 130 Td	Abundance (%) at 80 Td	Abundance (%) at 130 Td	Abundance (%) at 80 Td
trans-caryophyllene (Sigma-Aldrich, ≥98.5%)	41.04 ($C_3H_5^+$)	1.0	1.6	0.5	0.8
	69.07 ($C_5H_9^+$)	1.7	–	1.3	–
	81.07 ($C_6H_9^+$)	9.7	5.4	7.5	4.1
	95.09 ($C_7H_{11}^+$)	11.2	10.1	9.0	7.8
	109.10 ($C_8H_{13}^+$)	10.0	9.4	8.9	8.0
	121.10 ($C_9H_{13}^+$)	3.2	2.5	3.0	2.3
	123.12 ($C_9H_{15}^+$)	6.2	6.1	5.9	5.6
	135.12 ($C_{10}H_{15}^+$)	6.7	6.2	6.6	5.8
	137.13 ($C_{10}H_{17}^+$)	7.1	6.7	7.0	6.3
	149.13 ($C_{11}H_{17}^+$)	12.5	11.3	12.9	11.2
	205.20 ($C_{15}H_{25}^+$)	29.0	38.5	35.4	45.5
	221.19 ($C_{15}H_{25}O^+$)	1.7	2.2	2.0	2.6

and acyclic monoterpenes were prone to more fragmentation inside the drift tube. *p*-Cymene was the only monoterpenoid with the most abundant product ion of $C_7H_9^+$ at *m/z* 93.07. This was due to the stable aromatic ring structure of *p*-cymene that prevented further fragmentation. Another consequence of this stable molecular structure was very low fragmentation of *p*-cymene under lower reduced electric field conditions in the drift tube (E/N = 80 Td).

Protonated molecule clustering with water was observed for three monoterpenes: δ-limonene, 3-carene and sabinene. This is evidenced by the presence of ions at *m/z* 151.11 ($C_{10}H_{15}O^+$), and 153.13 ($C_{10}H_{17}O^+$) (Table 1). As Table 1 shows, especially δ-limonene clearly clustered with water molecule; the cluster ion detected at *m/z* 151.11 contributed 7.2% at 130 Td and 9.4% at 80 Td, and the cluster ion at *m/z* 153.13 contributed 5.9% at 130 Td and 8.0% at 80 Td from the total corrected cps of δ-limonene. Clustering of water with protonated molecules of sabinene and 3-carene was detected only at *m/z* 151.11 and the contribution of this water cluster was approximately less than 2.0% at 130 Td and over 2.0% at 80 Td from total corrected cps for both compounds, as can be seen from Table 1. This feature was independent from the monoterpene structure because these three compounds represent both mono- and bi-cyclic monoterpenes.

All sesquiterpenes produced one major product ion, $C_{11}H_{17}^+$, at *m/z* 149.13. All sesquiterpenes produced similar product ions, but the abundances of product ions were different depending on the molecular structure of the sesquiterpene. Tricyclic sesquiterpenes (aromadendrene and longifolene) exhibited a small degree of fragmentation compared to bicyclic (trans-caryophyllene) and monocyclic (α-humulene) sesquiterpene structures. Over 65% of the total corrected ion counts of tricyclic sesquiterpenes were detected at the protonated molecule ($C_{15}H_{25}^+$, *m/z* 205.20) and its isotope (*m/z* 206.20) at 130 Td, and over 80% at 80 Td. Clustering of protonated molecule of sesquiterpenes with water was observed with α-humulene, and *trans*-caryophyllene, whose water cluster at *m/z* 221.19 ($C_{15}H_{25}O^+$) contributed approximately 2.0% from the total corrected cps for both sesquiterpenes (Table 1). Moreover, at 80 Td we observed that protonated molecule of aromadendrene also clustered with water, producing the same water cluster at *m/z* 221.19 ($C_{15}H_{25}O^+$) that was observed for α-humulene, and *trans*-caryophyllene at both E/N settings. This water cluster of aromadendrene contributed 1.1% from the total corrected cps of aromadendrene. Longifolene did not demonstrate protonated molecule clustering with water. For both monoterpenes and sesquiterpenes (excluding *p*-cymene), the major product ion

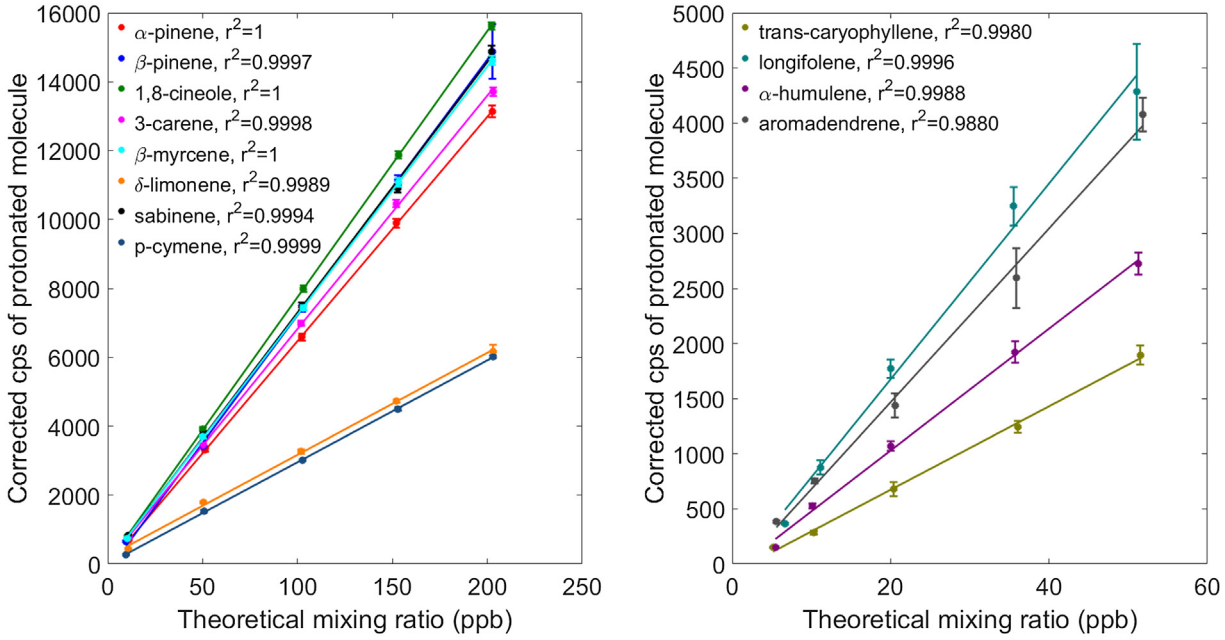

Fig. 5. Corrected cps of protonated molecule as a function of theoretical mixing ratio (calculated using Eq. (2)) for monoterpenes and monoterpene derivatives (left panel), and for sesquiterpenes (right panel). For 1,8-cineole the product ion $C_{10}H_{17}^+$ was used in the plot instead of the protonated molecule, due to its great degree of fragmentation (see Table 1). Error bars represent 1 standard deviation. Corrected cps was calculated as a 15 min average.

was produced by subtraction of the same neutral fragment, C_4H_8 (56 amu). For monoterpenes, this product ion appears at m/z 81.07 ($C_6H_9^+$) and for sesquiterpenes at m/z 149.13 ($C_{11}H_{17}^+$). According to Kim et al. this can be explained by Field's rule, which states that an intermediate proton-bound complex should dissociate preferentially to form a neutral that has a lower proton-affinity [9,32].

The fragmentation of mono- and sesquiterpenes in the PTR-ToF-MS produced similar product ions as previously reported for the PTR-Q-MS [8,9] with some notable differences. For 3-carene and sabinene, we observed that a small amount (approximately 2.0% from the total corrected cps) of $C_{10}H_{15}O^+$ (m/z 151.11) was formed as a result of protonated molecule clustering with water at both E/N settings. We also observed that δ-limonene was clustering with water producing $C_{10}H_{15}O^+$ (m/z 151.11) and $C_{10}H_{17}O^+$ (m/z 153.13) ions. Previously Tani et al. observed some formation of the protonated molecule–water cluster $C_{10}H_{19}O^+$ at m/z 155 for 3-carene and limonene using the PTR-Q-MS [8]. This different fragmentation behavior of formed protonated molecule–water clusters between the PTR-ToF-MS and the PTR-Q-MS can be related to different E/N settings between the two studies; we used 130 Td with the PTR-ToF-MS and Tani et al. used 120 Td with the PTR-Q-MS [8]. In addition to different water clusters of protonated molecules, we also observed other small differences in product ion distributions with monoterpenes compared to those previously reported with the PTR-Q-MS. For all monoterpenes we clearly observed the formation of a product ion $C_7H_9^+$ at m/z 93.07 that was speculated by Tani et al. to be one of the fragments of α-pinene, but was masked by impurities in their standard [8]. However, in our experiments this ion had similar behavior as the other product ions, and for each concentration studied this ion contributed with the same abundance to total corrected cps. Therefore, we believe that the ion $C_7H_9^+$ at m/z 93.07 was not produced by impurities, but due to fragmentation of the protonated molecule. With δ-limonene we observed two product ions that were not reported previously with PTR-Q-MS: $C_7H_9^+$ at m/z 93.07 and $C_8H_{11}^+$ at m/z 107.09. For sesquiterpenes we observed identical product ions as Kim et al. that were produced due to fragmentation of protonated molecule. In addition to product ions reported by Kim et al. [9], we observed that α-humulene, aromadendrene, and *trans*-caryophyllene produced a product ion $C_9H_{13}^+$ at m/z 121.10. Moreover, we observed that, as a result of fragmentation of α-humulene and *trans*-caryophyllene, product ions $C_3H_5^+$ at m/z 41.04 and $C_5H_9^+$ at m/z 69.07 were formed. All these three product ions ($C_9H_{13}^+$, $C_5H_9^+$, $C_3H_5^+$) were previously observed by Demarcke et al. with the PTR-Q-MS for α-humulene [10]. Additionally, we observed that α-humulene and *trans*-caryophyllene at both E/N settings, and aromadendrene at 80 Td, were clustering with water to produce a small amount of $C_{15}H_{25}O^+$ ions at m/z 221.19, as Table 1 shows. This protonated molecule clustering with water was not reported for the PTR-Q-MS [9,10].

The observed product ions in the PTR-ToF-MS were similar to the product ions reported in the PTR-Q-MS, but there were some notable differences that we will highlight here. We include a comparison of both the uncorrected and corrected product ion distributions where the "corrected" values have accounted for known differences in ion transmission efficiency between the two instruments. We acknowledge that a direct comparison between instruments using the uncorrected product ion distributions is not useful on its own, but when combined with the comparison of the corrected product ion distributions, can provide context for how much of the variation between the two instruments can be attributed to differences in transmission efficiency versus other sources. As expected, differences between the product ion distributions for the PTR-Q-MS and the PTR-ToF-MS were significant for the uncorrected signal values. For example, with the PTR-Q-MS at 120 Td Tani et al. reported that 43% from total uncorrected signal values of limonene was detected with its protonated molecule at m/z 137 [8]. We observed only 34.6% from total uncorrected signal values of limonene with its protonated molecule. Moreover, for 3-carene the fraction of protonated molecule from total uncorrected signal values was much closer to each other between these two instruments. Tani et al. reported that 58% from the total uncorrected signal values was detected with 3-carenes protonated molecule, whereas in our study we observed that 56.4% from the total uncorrected signal values was related to protonated molecule of 3-carene [8]. For sesquiterpenes the differences in fraction of protonated molecule (m/z 205) from total uncorrected signal values was significantly greater than with monoterpenes between the PTR-ToF-MS and the PTR-Q-MS. For example, Kim et al. reported with the PTR-Q-MS at 117 Td that only 10% from total uncorrected signal values of β-caryophyllene was detected with its protonated molecule, while we observed that protonated molecule of β-caryophyllene contributed 35.4% from its total uncorrected signal values [9]. The significant differences were observed also with other sesquiterpenes, for instance with aromadendrene Kim et al. reported that 34% from total uncorrected signal values was detected with protonated molecule of aromadendrene, whereas we observed that 72.3% from total uncorrected signal values of aromadendrene was detected with its protonated molecule. However, after correcting for the transmission efficiency of ions through the instruments, there were still notable differences in the product ion distributions. We were only able to compare corrected product ion distributions for sesquiterpenes from Kim et al. [9] and Demarcke et al. [10] because we could not locate product ion distributions for monoterpenes that had been corrected for transmission efficiency. The sesquiterpene datasets we used for comparison was collected with a PTR-Q-MS at similar drift tube settings at 117 Td by Kim et al. and at 130 Td by Demarcke et al. [9,10]. These ion distributions were compared to the values we measured with a PTR-ToF-MS at 130 Td. We observed that the abundance of protonated molecule corrected cps values from total corrected cps values with sesquiterpenes still differed between the PTR-Q-MS and the PTR-ToF-MS measurements, even though the cps values were corrected for instrument transmission coefficients. After transmission correction Kim et al. reported that protonated molecule of aromadendrene (m/z 205) covered 72% from its total ion signal, whereas we observed that it only covered 66.8% from its total ion signal after transmission efficiency of ions was corrected [9]. For longifolene Demarcke et al. reported that 65% from its total ion signal was covered by the protonated molecule, but as we show in Table 1 we observed that the protonated molecule of longifolene covered 70.6% from its total ion signal after transmission correction [10]. The variation in transmission corrected cps values was also observed with α-humulene and β-caryophyllene between two instruments at 130 Td. When measured by the PTR-Q-MS the protonated molecule of α-humulene contributed 48.5%, and protonated molecule of β-caryophyllene contributed 32% from total ion signal [10]. With the PTR-ToF-MS, the fraction of the protonated molecule of α-humulene was 43.6% and protonated molecule of β-caryophyllene was 29% from total ion signal. For monoterpenes we did not find product ion distributions calculated from transmission corrected cps in the previously published literature, so a similar comparison was not possible. However, based on differences observed with sesquiterpenes it is likely that there are also differences in monoterpene product ion distributions between the PTR-ToF-MS and the PTR-Q-MS even after transmission correction. The comparison of the transmission corrected signal abundances of the protonated molecules of sesquiterpenes shown above demonstrated not only that even after the transmissions correction there exist differences between the PTR-Q-MS and the PTR-ToF-MS, but the comparison also showed that this difference varies between sesquiterpenes. This variation indicates that it is difficult to estimate the real product ion dis-

tribution, if it has not been determined for the instrument with right mass analyzer. Consequently, the difference that still exists in the abundance of protonated molecule cps from total cps after the transmission correction highlights the need for the product ion distributions of several mono-and sesquiterpenes, reported for the time-of-flight mass spectrometer.

3.4. PTR-ToF-MS response to mono- and sesquiterpenes under varying range of humidity

The humidity-dependent response of the PTR-ToF-MS was investigated for three different compounds: α-pinene, δ-limonene, and longifolene. The RH was adjusted by varying the ratio of humid and dry dilution air. This approach allowed us to investigate humidity-dependent responses from 0% to 60% RH with the dynamic dilution system. Results are presented in the upper panel of Fig. 6. δ-Limonene exhibited a small humidity-dependence. Fig. 6 illustrates that for the protonated molecule of δ-limonene, there was an increase from 29% to 33% with increasing humidity. Similarly, for α-pinene no humidity-dependence was observed, as shown in Fig. 6. These results are in agreement with the results reported earlier by Tani et al. using the PTR-Q-MS [8,15]. For the protonated molecule of δ-limonene, Tani et al. reported an increase of 4% (from 42% to 46%) at 122–124 Td, when RH was varied from 0% to 100% [8]. For protonated molecule of α-pinene Tani et al. reported only a small increase of 1% (from 47% to 48%) at 122–124 Td, when RH was increased from 0% to 100% [15]. For the protonated molecule of longifolene we observed an increase from 56% to 60%, across the RH range (Fig. 6). The humidity dependent response of the PTR-Q-MS to longifolene has been reported earlier by Demarcke et al. in a very limited range of humidity (0.61 kPa-1.01 kPa) [10]. They reported that the response of the PTR-Q-MS to longifolene was only slightly affected (from 64% to 65%) by humidity in this range [10]. Hence, we observed a stronger effect of humidity on longifolene detection by the PTR-ToF-MS with the dynamic dilution system, but the studied RH range was wider in our experiments. These humidity-dependent tests show that the response of the PTR-ToF-MS to detect mono- and sesquiterpenes with their protonated molecule is slightly humidity dependent for some compounds, but not for all. Only slight humidity-dependence was observed, even if the relative abundance of the primary ion (H_3O^+, mass 19 in the lower panel of Fig. 6) decreased as a function of RH from 96.5% to 70.5%. At the same time the relative abundances of the clusters of primary ions ($H_3O^+(H_2O)$, $H_3O^+(H_2O)_2$, masses 37 and 55 in the lower panel of Fig. 6) increased from 3.5% to 29% (mass 37) and 0% to 0.5% (mass 55). The reason for the minor effect of increasing RH on α-pinene and δ-limonene detection is that these compounds have higher proton affinities than water (691 kJ/mol) or water dimer ($(H_2O)_2$, 808 kJ/mol) which were present in substantial amounts in the drift tube during these experiments [3,16,33]. Due to the high proton affinity, α-pinene and δ-limonene can go through direct proton transfer with $H_3O^+(H_2O)$ ion in addition to H_3O^+ ion, resulting in a minor effect of increasing humidity on the detection of these compounds with their protonated molecules. For longifolene the proton affinity is not available, but the similar humidity dependence of longifolene, α-pinene and δ-limonene suggests that longifolene also has a higher proton affinity than the water dimer. Overall, the humidity-dependent response of the PTR-ToF-MS was fairly minor across the RH range even for the compounds that exhibited a humidity dependent response. Therefore, humidity differences between measurement versus calibration conditions would not contribute to an important source of measurement uncertainty in the PTR-ToF-MS. Moreover, these results were in agreement with earlier studies conducted with a PTR-Q-MS suggesting that the type of mass analyzer used for the PTR-MS has limited effect on the humidity-dependent response of the PTR-MS.

3.5. Implications for ambient BVOC measurements

PTR-ToF-MS is frequently used to measure BVOCs emissions from vegetation or BVOC concentrations in the ambient atmosphere. Vegetation emits thousands of different BVOCs representing a range of different isomers that are not distinguishable with the PTR-MS. Our results have demonstrated that the degree of fragmentation of monoterpenes and sesquiterpenes inside the PTR-ToF-MS depend on their structures, and can be substantially different between isomers. Therefore, it is crucial to know exactly which mono- and sesquiterpenes are measured with the PTR-ToF-MS, and calibrate the instrument for those specific compounds. The identification of mono- and sesquiterpenes can be accomplished by employing a set of complementary analytical techniques. For example, terpenoid isomers can be identified with offline GC–MS analysis techniques. Neglecting to account for different product ion distributions from different isomers can lead to significant quantification error with the PTR-MS. To demonstrate the magnitude of this effect, we calculated the quantification errors for a realistic mixture of BVOCs using the product ion distributions for corrected cps values shown in left side of Table 1. For the calculations we used two example cases to demonstrate the possible scenarios the PTR-MS user could face during the measurements and data analysis, especially in an environment where the emission profiles are unknown. Example case 1 is representative of an emission profile from blue spruce (*Picea pungens)* where total monoterpenes are dominated by three compounds including 14% α-pinene, 34% limonene, and 21% β-myrcene [34]. For this monoterpene mixture, calculated monoterpene mixing ratios would have an error of over 17% if α-pinene fragmentation was assumed to represent the measured monoterpene emissions. Example case 2 represents the scenario where Scots pine (*Pinus sylvestris*) emissions of sesquiterpenes change due to seasonal variation. Scots pines can substantially increase their emission of β-caryophyllene due to seasonal variation while emissions of other sesquiterpenes, such as longifolene, do not change [35]. An error of 26% for calculated sesquiterpene mixing ratios would result if instrument user assumes during quantification that the measured sesquiterpenes included 50% longifolene and 50% β-caryophyllene during the whole measurement period, but actually due to change in emission profile sesquiterpenes included 95% β-caryophyllene and only 5% longifolene at the end of the measurements. Therefore, in the case of sesquiterpenes the quantification error due to wrong emission profile assumptions could be even more significant than with monoterpenes. The importance of knowing the terpene profile of the environment where PTR-MS measurements are conducted was previously highlighted by Joo et al. [36]. They showed that linalool that fragments largely to the *m*/*z* 137 in the PTR-MS can cause an increase up to a factor of 2 for the measured monoterpene emission rates, if monoterpenes are monitored only with ion signal at *m*/*z* 137, and the knowledge about the emission profile is missing. Therefore, they also emphasized in their study that a lack of knowledge about the composition of terpenoids measured can lead to erroneous quantitation by PTR-MS, and suggested to supplement PTR-MS measurements with regular GC–MS measurements to avoid the quantification errors caused by missing knowledge about the emission profile measured. These example cases highlight the necessity of the identification of the terpenoid compounds measured by the PTR-ToF-MS. After the identification, the instrument can be calibrated using the correct compounds in order to avoid significant quantification errors caused by different product ion distributions of different compounds.

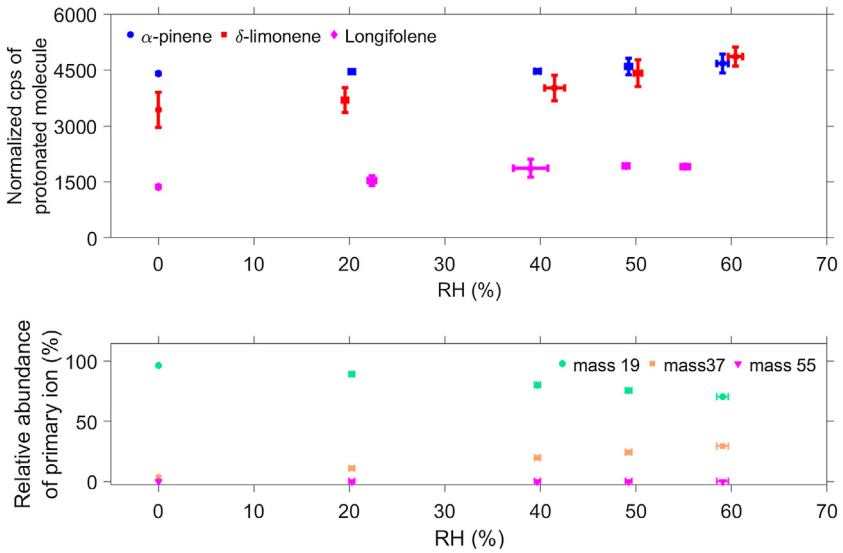

Fig. 6. Normalized cps as a function of RH for protonated molecules of α-pinene (100 ppb), δ-limonene (100 ppb), and longifolene (35 ppb) (upper panel). Relative abundance of primary ion and its clusters as a function of RH during α-pinene experiment (lower panel). Error bars represent 1 standard deviation of 10-min average. Normalized cps has been taken as 10 min' averages.

4. Conclusions

The PTR-MS response to VOCs depends on different factors, including how effectively the instrument can collect and detect measured VOC, and on the extent to which the reactions between H_3O^+ ions and VOCs are occurring in the drift tube. Moreover, the PTR-MS is commonly operated at high E/N values to minimize clustering of the reagent and product ions with water, but it promotes increased fragmentation of many trace VOCs due to the increased number of energetic collisions occurring inside the drift tube. Therefore, accurate quantification of VOC mixing ratios requires the calibration of the PTR-MS under the operating conditions. We used a dynamic dilution system to characterize PTR-ToF-MS analysis of BVOCs—including PTR-MS calibration, investigation of BVOC product ion distributions, and humidity-dependent BVOC responses. Using this system, we reported the product ion distributions of several mono- and sesquiterpenes for the PTR-ToF-MS for two E/N values, 130 Td and 80 Td. This is the first report, to our knowledge, of this valuable information for the PTR-ToF-MS. We have demonstrated that the structure of terpenoid compounds has a substantial impact on its product ion distribution. This is especially true with high E/N settings that are commonly used during normal PTR-MS operation to decrease the clustering of the reagent and product ions with water. In this work we showed that the product ion distributions of mono- and sesquiterpenes determined for the PTR-ToF-MS differed from the ones determined for the PTR-Q-MS, even after the transmission corrected product ion distributions of sesquiterpenes were compared. Therefore, these distributions offer an important piece of information for PTR-ToF-MS users who are quantifying BVOC emissions from vegetation and ambient BVOC concentrations. Furthermore, we demonstrated with three compounds that the PTR-ToF-MS response to protonated molecules of mono- and sesquiterpenes did exhibit only a small humidity-dependence across a large RH range from 0% to 60%. We determined that performing the measurements in wet environment can increase the response of the PTR-ToF-MS to protonated molecule of mono- and sesquiterpenes by 4%, compared to dry environment. Therefore, we further conclude that the humidity in which mono- and sesquiterpenes are measured with the PTR-ToF-MS will not contribute to an appreciable source of uncertainty to the PTR-ToF-MS measurements. Moreover, we have shown that significant measurement errors are likely to occur if the quantification of mono- or sesquiterpenes measured by the PTR-MS is done without information about the detailed terpene profiles. Our calculations demonstrate that ambient monoterpene measurements could have an error of 17% if the monoterpene complexity is ignored and α-pinene is assumed to dominate. Our calculations also demonstrate that the quantification error for sesquiterpenes could be off by more than 25% if the ambient profile is dominated by β-caryophyllene, but the product ion distribution is assumed to be equally contributed by β-caryophyllene and longifolene. To avoid quantification errors associated with differences in fragmentation between isomers, users should employ complementary analytical techniques. For example, off-line GC–MS analysis or some other method for identification of individual mono- and sesquiterpene isomers should always be available to supplement the PTR-MS measurements.

Acknowledgements

This work was financially supported by the European Research Council (ERC Starting Grant 335478) and The Academy of Finland Center of Excellence programme (grant no 307331). The work of E. Kari was financially supported by University of Eastern Finland Doctoral Program in Environmental Physics, Health and Biology.

References

[1] R.S. Blake, P.S. Monks, A.M. Ellis, Proton-transfer reaction mass spectrometry, Chem. Rev. 109 (2009) 861–896.
[2] J. de Gouw, C. Warneke, Measurements of volatile organic compounds in the earths atmosphere using proton-transfer-reaction mass spectrometry, Mass Spectrom. Rev. 26 (2007) 223–257.
[3] A.M. Ellis, C.A. Mayhew, Proton Transfer Reaction Mass Spectrometry: Principles and Applications, 1st ed., John Wiley & Sons Ltd, United Kingdom, 2014.
[4] S. Juran, E. Pallozzi, G. Guidolotti, S. Fares, L. Sigut, C. Calfapietra, A. Alivernini, F. Savi, K. Vecerova, K. Krumal, Z. Vecera, O. Urban, Fluxes of biogenic volatile organic compounds above temperate Norway spruce forest of the Czech Republic, Agric. For. Meteorol. 232 (2017) 500–513.
[5] W.J.F. Acton, S. Schallhart, B. Langford, A. Valach, P. Rantala, S. Fares, G. Carriero, R. Tillmann, S.J. Tomlinson, U. Dragosits, D. Gianelle, C.N. Hewitt, E. Nemitz, Canopy-scale flux measurements and bottom-up emission estimates of volatile organic compounds from a mixed oak and hornbeam forest in northern Italy, Atmos. Chem. Phys. 16 (2016) 7149–7170.
[6] L. Kaser, T. Karl, A. Guenther, M. Graus, R. Schnitzhofer, A. Turnipseed, L. Fischer, P. Harley, M. Madronich, D. Gochis, E.N. Keutsch, A. Hansel,

Undisturbed and disturbed above canopy ponderosa pine emissions: PTR-TOF-MS measurements and MEGAN 2.1 model results, Atmos. Chem. Phys. 13 (2013) 11935–11947.
[7] R. Taipale, T.M. Ruuskanen, J. Rinne, M.K. Kajos, H. Hakola, T. Pohja, M. Kulmala, Technical Note Quantitative long-term measurements of VOC concentrations by PTR-MS—measurement, calibration, and volume mixing ratio calculation methods, Atmos. Chem. Phys. 8 (2008) 6681–6698.
[8] A. Tani, S. Hayward, C.N. Hewitta, Measurement of monoterpenes and related compounds by proton transfer reaction-mass spectrometry (PTR-MS), Int. J. Mass Spectrom. 223 (2003) 561–578.
[9] S. Kim, T. Karl, D. Helmig, R. Daly, R. Rasmussen, A. Guenther, Measurement of atmospheric sesquiterpenes by proton transfer reaction-mass spectrometry (PTR-MS), Atmos. Meas. Tech. 2 (2009) 99–112.
[10] M. Demarcke, C. Amelynck, N. Schoon, F. Dhooghe, H. Van Langenhove, J. Dewulf, Laboratory studies in support of the detection of sesquiterpenes by proton-transfer-reaction-mass-spectrometry, Int. J. Mass Spectrom. 279 (2009) 156–162.
[11] X.B. Pang, Biogenic volatile organic compound analyses by PTR-TOF-MS: calibration, humidity effect and reduced electric field dependency, J. Environ. Sci.—China 32 (2015) 196–206.
[12] T.M. Ruuskanen, M. Mueller, R. Schnitzhofer, T. Karl, M. Graus, I. Bamberger, L. Hortnagl, F. Brilli, G. Wohlfahrt, A. Hansel, Eddy covariance VOC emission and deposition fluxes above grassland using PTR-TOF, Atmos. Chem. Phys. 11 (2011) 611–625.
[13] C.L. Faiola, M.H. Erickson, V.L. Fricaud, B.T. Jobson, T.M. VanReken, Quantification of biogenic volatile organic compounds with a flame ionization detector using the effective carbon number concept, Atmos. Meas. Tech. 5 (2012) 1911–1923.
[14] M. Graus, M. Muller, A. Hansel, High resolution PTR-TOF: quantification and formula confirmation of VOC in real time, J. Am. Soc. Mass Spectrom. 21 (2010) 1037–1044.
[15] A. Tani, S. Hayward, A. Hansel, C.N. Hewitt, Effect of water vapour pressure on monoterpene measurements using proton transfer reaction-mass spectrometry (PTR-MS), Int. J. Mass Spectrom. 239 (2004) 161–169.
[16] W. Lindinger, A. Hansel, A. Jordan, On-line monitoring of volatile organic compounds at pptv levels by means of proton-transfer-reaction mass spectrometry (PTR-MS)—Medical applications, food control and environmental research, Int. J. Mass Spectrom. 173 (1998) 191–241.
[17] L. Keck, U. Oeh, C. Hoeschen, Corrected equation for the concentrations in the drift tube of a proton transfer reaction-mass spectrometer (PTR-MS), Int. J. Mass Spectrom. 264 (2007) 92–95.
[18] J. de Gouw, C. Warneke, T. Karl, G. Eerdekens, C. van der Veen, R. Fall, Sensitivity and specificity of atmospheric trace gas detection by proton-transfer-reaction mass spectrometry, Int. J. Mass Spectrom. 223 (2003) 365–382.
[19] A. Hansel, W. Singer, A. Wisthaler, M. Schwarzmann, W. Lindinger, Energy dependencies of the proton transfer reactions H3O(+)+CH2O double left right arrow CH2OH++H2O, Int. J. Mass Spectrom. 167 (1997) 697–703.
[20] J. Brito, A. Zahn, An unheated permeation device for calibrating atmospheric VOC measurements, Atmos. Meas. Tech. 4 (2011) 2143–2152.
[21] A. Feilberg, D.Z. Liu, A.P.S. Adamsen, M.J. Hansen, K.E.N. Jonassen, Odorant emissions from intensive pig production measured by online proton-transfer-reaction mass spectrometry, Environ. Sci. Technol. 44 (2010) 5894–5900.
[22] K.B. Haase, W.C. Keene, A.A.P. Pszenny, H.R. Mayne, R.W. Talbot, B.C. Sive, Calibration and intercomparison of acetic acid measurements using proton-transfer-reaction mass spectrometry (PTR-MS), Atmos. Meas. Tech. 5 (2012) 2739–2750.
[23] J.P. Greenberg, H. Friedli, A.B. Guenther, D. Hanson, P. Harley, T. Karl, Volatile organic emissions from the distillation and pyrolysis of vegetation, Atmos. Chem. Phys. 6 (2006) 81–91.
[24] L. Fischer, A. Klinger, J. Herbig, K. Winkler, R. Gutmann, A. Hansel, The LCU: versatile trace gas calibration, in: 6th International Conference on Proton Transfer Reaction Mass Spectrometry and its Applications, Obergurgl, Austria, 2013, pp. 192–194.
[25] K.J. Jardine, W.M. Henderson, T.E. Huxman, L. Abrell, Dynamic Solution Injection: a new method for preparing pptv-ppbv standard atmospheres of volatile organic compounds, Atmos. Meas. Tech. 3 (2010) 1569–1576.
[26] G.D. Mitchell, A review of permeation tubes and permeators, Separ. Purif. Method 29 (2000) 119–128.
[27] B. Rappengluck, E. Apel, M. Bauerfeind, J. Bottenheim, P. Brickell, P. Cavolka, J. Cech, L. Gatti, H. Hakola, J. Honzak, R. Junek, D. Martin, C. Noone, C. Plass-Dulmer, D. Travers, D. Wang, The first VOC intercomparison exercise within the global atmosphere watch (GAW), Atmos. Environ. 40 (2006) 7508–7527.
[28] E.C. Apel, J.G. Calvert, T.M. Gilpin, F.C. Fehsenfeld, D.D. Parrish, W.A. Lonneman, The nonmethane hydrocarbon intercomparison experiment (NOMHICE): task 3, J. Geophys. Res.—Atmos. 104 (1999) 26069–26086.
[29] A. Jordan, S. Haidacher, G. Hanel, E. Hartungen, L. Mark, H. Seehauser, R. Schottkowsky, P. Sulzer, T.D. Mark, A high resolution and high sensitivity proton-transfer-reaction time-of-flight mass spectrometer (PTR-TOF-MS), Int. J. Mass Spectrom. 286 (2009) 122–128.
[30] C. Warneke, C. van der Veen, S. Luxembourg, J.A. de Gouw, A. Kok, Measurements of benzene and toluene in ambient air using proton-transfer-reaction mass spectrometry: calibration, humidity dependence, and field intercomparison, Int. J. Mass Spectrom. 207 (2001) 167–182.
[31] J.r.H. Gross, Mass Spectrometry: A Textbook, 2nd ed., Springer, Berlin; New York, 2010.
[32] F.W. McLafferty, F.E. Tureček, Interpretation of Mass Spectra, 4th ed., University Science Books, Mill Valley, Calif, 1993.
[33] M.T. Fernandez, C. Williams, R.S. Mason, B.J.C. Cabral, Experimental and theoretical proton affinity of limonene, J. Chem. Soc. Faraday Trans. 94 (1998) 1427–1430.
[34] C.L. Faiola, B.T. Jobson, T.M. VanReken, Impacts of simulated herbivory on volatile organic compound emission profiles from coniferous plants, Biogeosciences 12 (2015) 527–547.
[35] V. Tarvainen, H. Hakola, H. Hellen, J. Back, P. Hari, M. Kulmala, Temperature and light dependence of the VOC emissions of Scots pine, Atmos. Chem. Phys. 5 (2005) 989–998.
[36] E. Joo, J. Dewulf, M. Demarcke, C. Amelynck, N. Schoon, J.F. Muller, M. Simpraga, K. Steppe, H. Van Langenhove, Quantification of interferences in PTR-MS measurements of monoterpene emissions from Fagus sylvatica L. using simultaneous TD-GC–MS measurements, Int. J. Mass Spectrom. 291 (2010) 90–95.